


 Cite this: *Phys. Chem. Chem. Phys.*, 2022, 24, 17956

 Received 31st March 2022,
Accepted 13th July 2022

DOI: 10.1039/d2cp01496c

rsc.li/pccp

Binary mono-anions with unprecedented anti-aromatic planar tetracoordinate carbon and nitrogen atoms†

 Bo Jin * and Zai-Ran Wang

Global minima (CBe₄⁻ and NBe₄⁻) with planar tetracoordinate carbon and nitrogen atoms are stabilized by multicentric bonds. Their unusual anti-aromaticity is due to the strong localized Be–Be bonds preventing the full delocalization of the electrons in the CBe₄/NBe₄ skeleton. These binary mono-anions are expected to be experimentally realized in the gas phase.

Having two electrons in four valence orbitals, beryllium prefers multicentre bonding owing to this typical electron deficiency, and is suitable for use as a key ligand atom to construct a planar hypercoordinate carbon (phC) cluster.¹ Here phC denotes a kind of exotic carbon that conflicts with the most important paradigms from the long-standing tetrahedral model of van't Hoff and Lebel in organic chemistry. After nearly half a century of exploration, the coordination numbers of phCs have increased from the initial 4 to 7. In addition, the central atom was not limited to carbon, and covered almost all main group elements in the second period except lithium and gradually extended to elements of higher periods.^{1,2} Regrettably, most of them were computationally designed, and experimentally synthesizing them is still very difficult except for a few. Specifically, thermodynamically favorable global minima (GM) are most likely to be experimentally detected according to Boltzmann's law of distribution, which has been confirmed by results from joint experimental and computational studies.³ Therefore, designing GM of exotic planar species on their potential energy surfaces has become the consensus of all theoretical chemists.

Negative ion photoelectron spectroscopy⁴ (PES) is the most widely used experimental tool to characterize these unusual planar clusters realized by laser vaporization. In 1999, Wang

and Boldyrev *et al.* characterized the first planar tetracoordinate carbon (ptC) CAI₄⁻ by combining PES experiments and theoretical calculations. Then, SiAl₄⁻ and GeAl₄⁻, the isoelectron clusters of CAI₄⁻, were also reported in 2000.⁵ At the same time, Rao *et al.* also experimentally observed the planar tetracoordinate nitrogen (ptN) NAl₄⁻ predicted by Schleyer and Boldyrev in 1991.⁶ Remarkably, the star-like ptC cluster C₅Al₅⁻ predicted by Wu's group in 2011 was recently realized experimentally by Zhang *et al.*⁷ The PES experimental technique, however, also has significant limitations, and generally only mono-anionic species with simple components (as mentioned earlier) are detected by it among a large number of predicted planar clusters. In particular, more than half of the theoretical predictions for planar pentacoordinate carbons are beryllium related,^{1,8} but these clusters have not been hitherto detected experimentally. This is admittedly due to the high toxicity of beryllium and its compounds, but its' complex components (ternary even quaternary), or do not meet the harsh conditions of the mono-anion that is the main reason for its unattainability. Consequently, in addition to satisfying GM of clusters, theoretical chemists are also asked to design mono-anions and make sure that their composition is as uncomplicated as possible.

Aromaticity⁹ is one of the central concepts of chemistry and is important for the low energy and stability of ring-closed conjugated systems. Usually, the number of delocalized electrons in aromatic systems meets Hückel's 4*n* + 2 rule. In particular, π aromaticity is crucial for maintaining the stability of these planar clusters. In addition, their electron-deficient ligand atoms frequently meet the requirement of σ-donating and π-accepting, thus making these planar clusters possess σ and π double aromaticity.^{1,8,10} In contrast, anti-aromaticity⁹ is generally used to describe an effect in which the departure of delocalized electrons leads to an increase in energy and a decrease in stability of the system, and these clusters have 4*n* delocalized electrons. Herein, one would wonder: can planar hypercoordination be constructed by beryllium ligands alone? Are these clusters necessarily aromatic? In this work, we report

Institute of Molecular Science, Shanxi University, Taiyuan, 030006, People's Republic of China. E-mail: 201722802002@email.sxu.edu.cn

† Electronic supplementary information (ESI) available: Relative energies of 1 and 2 and the corresponding isomers, iso-chemical shielding surfaces (ICSSs) of 1 and 2, the NICS_{zz} values of benzene, simulated PES spectra of 1 and 2, and Cartesian coordinates for the species reported in this work. See DOI: <https://doi.org/10.1039/d2cp01496c>

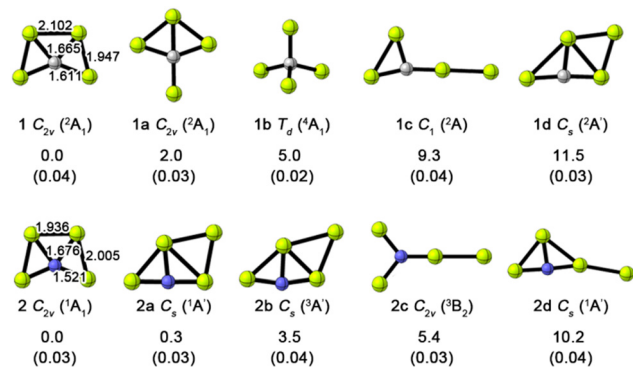


Fig. 1 B3LYP/aug-cc-pVTZ-optimized structures of CBe₄⁻ (**1**), NBe₄⁻ (**2**), and the corresponding isomers. The interatomic distances are given in Å. The relative energies (Δ*E*, in kcal mol⁻¹) are reported at the CCSD(T) + ZPE_{B3LYP} level. *T*₁ diagnostic values are given within parentheses.

two binary mono-anionic clusters CBe₄⁻ and NBe₄⁻, which contain a planar tetracoordinate carbon and nitrogen atom, respectively. Unusually, these clusters are anti-aromatic. It is worth noting that we have previously reported on ptC cluster CBe₄²⁻,¹¹ although it is a dynamically stable GM constructed by beryllium ligands alone, its higher valence state (negative divalent does not satisfy the requirement of a mono-anion) is not favorable for experimental observation of PES.

As shown in Fig. 1, the clusters CBe₄⁻ (**1**, ²A₁) and NBe₄⁻ (**2**, ¹A₁) adopt the high symmetry of C_{2v} at the B3LYP/aug-cc-pVTZ level using the Gaussian 16 package.¹² The Be–C distances in **1** are 1.665 and 1.611 Å. They are very close to the standard Be–C single bond lengths (sum of covalent radii of Be and C atoms, being 1.77 Å).¹³ Similarly, the Be–N distances in **2** are 1.676 and 1.521 Å, which are close to Be–N single bond lengths (1.73 Å). Therefore, **1** and **2** are the qualified ptC and ptN clusters. An extensive exploration (doublet and quartet for **1**, singlet and triplet for **2**) of their potential energy surfaces (PESs) using a stochastic search algorithm¹⁴ indicates that **1** and **2** are GMs. They are 2.0 and 0.3 kcal mol⁻¹ lower in energy than their corresponding second lowest isomers (see Fig. 1), respectively, where the relative energies of the low-lying isomers were calculated at the CCSD(T)/aug-cc-pVTZ level and corrected with the B3LYP/aug-cc-pVTZ zero-point energies. Noteworthily, **2a** and **2** are extremely close in energy, so the former is deemed as an isoenergetic isomer of the latter, and they are most likely to be observed simultaneously in the experiment. Since these clusters (Fig. 1) have slightly higher *T*₁ diagnostic values, we performed multi-reference configuration interaction (MRCI)¹⁵ calculations to confirm that the single reference-based method is adequate to describe these systems. As shown in Fig. S1 (ESI[†]), **1**, **1a**, and **1b** are very close in energy, and these are competitive isomers that may be observed experimentally; cluster **2** is low in energy, compared to other isomers and is a true GM. This result is not significantly different from the present single-reference system.

Examining whether these thermodynamically stable GMs **1** and **2** are dynamically stabilized is a key for the experimental realization. To this end, the 50 pico-second (ps) Born–Oppenheimer

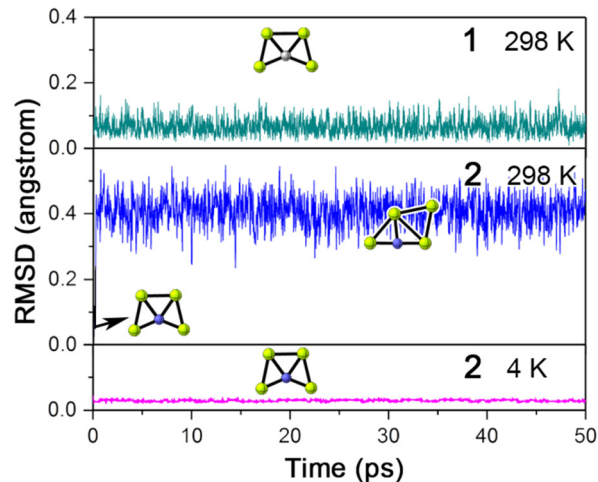


Fig. 2 RMSD (in Å) versus simulation time (in ps) for the BOMD simulations of CBe₄⁻ (**1**) and NBe₄⁻ (**2**) at the PBE/DZVP level and 298 and 4 K.

molecular dynamic (BOMD)¹⁶ simulations were performed at the PBE/DZVP level and concerned temperatures. The result of simulations is described by the root-mean-square derivation (RMSD, in Å) relative to the PBE/DZVP-optimized structures to evaluate the dynamic stability of **1** and **2**. As shown in Fig. 2, the RMSD plot of **1** at 298 K has no meaningful upward jump, its fluctuation is very gentle, and is reflected in a small average RMSD value (0.066 Å). Nevertheless, the RMSD plot for **2** at the same temperature has an irreversible upward jump soon after the simulations start, suggesting irreversible isomerization. Sampling its structure demonstrates that it is isomer **2a**. Although the result indicates that **2** is unstabilized at room temperature different from **1**, it has the possibility to be realized at cryogenic temperatures. At the bottom of Fig. 2, the RMSD plot of **2** at 4 K is smooth, with hardly any fluctuations, which indicates its high dynamic stability.

The analysis of the electronic structures of these clusters gives the reason for their stability. In this regard, the adaptive natural density partitioning (AdNDP) program¹⁷ is a powerful tool, which helps in analysing the bonding with *n*-center two electron (*nc*-2e) pairs in an unknown cluster. The AdNDP results for **1** and **2** are shown in Fig. 3. For open-shell cluster **1**, it has 13 valence electrons, in which one is the Be–Be 2c-1e σ bond (element **A**) with an occupation number (ON) of 0.94 |e|, and two pairs are Be–Be 2c-2e σ bonds (element **B** and **C**, ON = 1.81 |e|). The remaining four pairs are related to the central C atom, which forms four sets of multicentric bonds, including three 5c-2e σ bonds (element **D–F**, ON = 2.00 |e|) and one 5c-2e π bond (element **G**, ON = 2.00 |e|). The bonding of **2** is essentially similar to that of **1** and also involves the four 5c-2e bonds (element **K–N**, ON = 2.00 |e|) and these multicentric bonds are the main reason for maintaining the stability of these planar species. Moreover, compared with the one Be–Be 2c-1e σ bond (element **A**) between the top two Be atoms in **1**, the Be–Be bond in **2** is a 2c-2e σ bond (element **H**, ON = 1.97 |e|), which explains the longer Be–Be distance in **1** than in **2** (2.102 vs. 1.936 Å).

Normally, these four delocalized σ/π bonds in **1** and **2** are in compliance with Hückel's rule, which offers double 6σ/2π

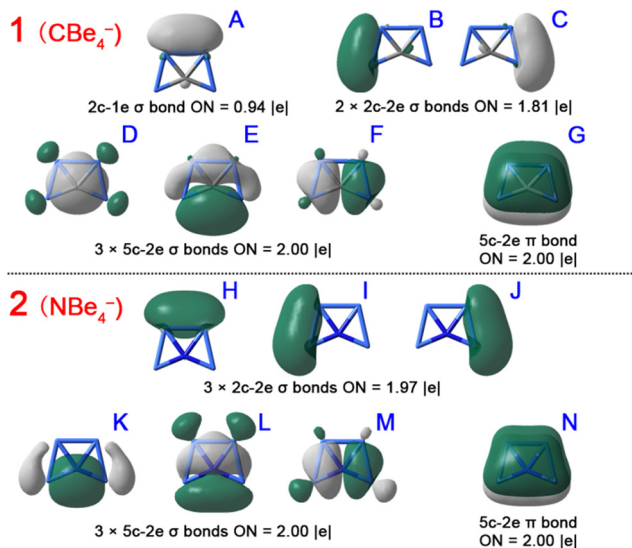


Fig. 3 AdNDP bonding patterns of CBe_4^- (**1**), and NBe_4^- (**2**). Occupation numbers (ONs) are denoted.

aromaticity to them. Interestingly, we achieved the exact opposite result by evaluating their aromaticity, *i.e.*, **1** and **2** have unprecedented anti-aromaticity. As the most authoritative measure of aromaticity, the nucleus-independent chemical shift (NICS)¹⁸ calculations were performed. Compared with the qualitative Hückel rule, NICS gives quantitative aromatic intensity. As shown in Fig. 4a, except for the negative NICS_{zz} values (−23.7 and −11.4 ppm) at the center of the Be–C–Be triangle, all other examined points located within or above the molecule have notable positive NICS_{zz} values, which indicates the anti-aromaticity of the species **1**, and the NICS_{zz} result of **2** is also similar to that of **1**. We further used iso-chemical shielding

surfaces¹⁹ (ICSSs) for a more comprehensive analysis, and the result is given in the ESI† as Fig. S1. As shown in Fig. S2 (ESI†), except for the small chemical shielding region near the horizontally oriented Be–C–Be triangle and molecular outside, the vertical directions of the molecular bodies belong to de-chemical shielding regions with negative NICS_{zz} values, indicating that **1** and **2** are anti-aromatic. Moreover, we also provided the NICS_{zz} values for a representative aromatic molecule benzene as a standard reference.²⁰ As shown in Fig. S3 (ESI†), it has notable negative NICS_{zz} values (−16.1 to −30.0 ppm), which are clearly different from the larger positive NICS_{zz} values that clusters **1** and **2** have.

Why do clusters **1** and **2** show such perverse anti-aromaticity? Some clues are obtained by comparing the aromaticity of previously reported ptC clusters CBe_4^{2-} and CBe_4H_3^+ .¹¹ We recalculate their NICS values, the results are given in Fig. 4b. All examined points located within or above the molecule have notable positive NICS_{zz} values, indicating the anti-aromaticity of the cluster CBe_4^{2-} . In stark contrast, all examined points in CBe_4H_3^+ have negative NICS_{zz} values, which suggests it is aromatic. What caused this change from anti-aromatic CBe_4^{2-} to aromatic CBe_4H_3^+ ? Structurally, the latter has three H atoms at the periphery compared to the former. Reflecting on the bonding mode, the latter converts the former stronger localized Be–Be 2c-2e bond to the delocalized Be–H–Be 3c-2e bond. This makes the electrons on its CBe_4 skeleton fully delocalized, so that the latter is aromatic. In other words, the former highly localized Be–Be bond hinders the delocalization of electrons on the CBe_4 skeleton, making it anti-aromatic. Similarly, the clusters **1** and **2** reported in this paper have similar bonding patterns to CBe_4^{2-} and are therefore also anti-aromatic.

Since the binary anionic clusters **1** and **2** are the dynamically viable GMs with well-defined electronic structures, they are

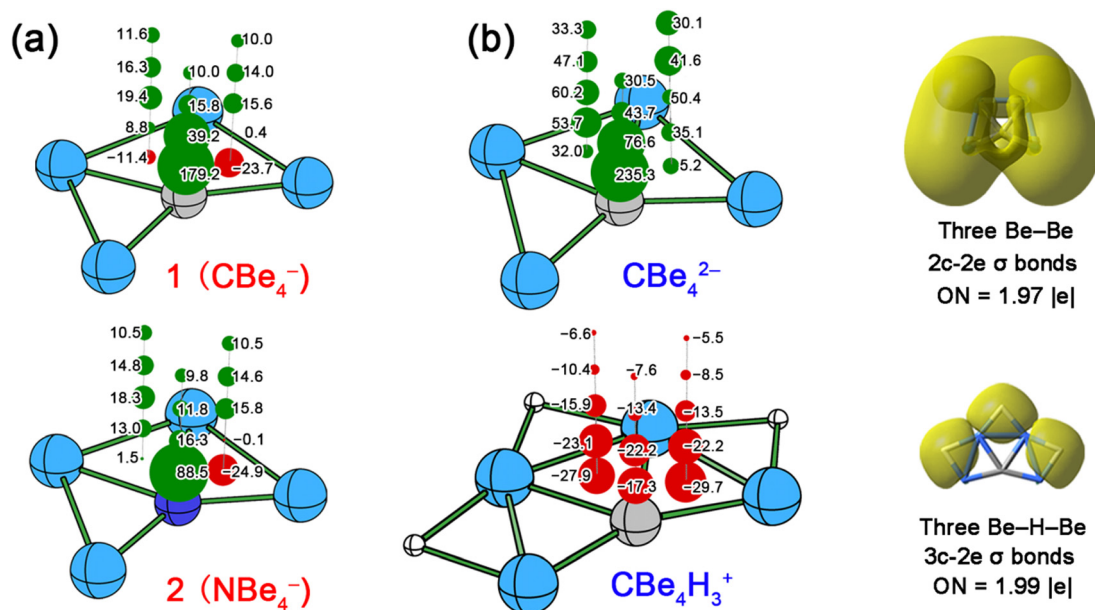


Fig. 4 NICS_{zz} values of **1** and **2** (a), and CBe_4^{2-} and CBe_4H_3^+ (b). Along the vertical lines, the NICS points (green, red balls) are 0.5 Å apart from their neighbors. Key AdNDP bonding patterns of CBe_4^{2-} and CBe_4H_3^+ (b).

promising for experimental realization in PES. To give the reference information for the experiments, the PES spectra of **1** and **2** have been simulated. The first vertical detachment energies (VDEs) were obtained by calculating the energy differences between anions and neutrals based on the anions' geometries at the CCSD(T)/aug-cc-pVTZ level. The VDEs, corresponding to the excited states of the neutrals, were calculated using a time-dependent (TD) procedure at the DFT B3LYP/aug-cc-pVTZ level. As shown in Fig. S4 (ESI[†]), clusters **1** and **2** possessed the first VDEs of 2.05 and 2.09 eV, respectively. The first VDEs themselves are seen as the most remarkable character of the PES spectra of **1** and **2**. In addition, other peaks in the spectra are seen as the fingerprints of **1** and **2**, and they can be recorded in the current PES spectra because the binding energies are lower than 6.40 eV, which is within the range of the machine. Furthermore, we calculated the adiabatic electron detachment energies (ADEs) of clusters **1** and **2**. The ADE value of cluster **2** (1.94 eV) is close to and slightly lower than its VDE value (2.09 eV). This indicates the rigidity of its structures. In contrast, the larger difference between the two corresponding energies for cluster **1** is larger (1.76 vs. 2.05 eV), indicating that its structure is easy to isomerize upon the loss of one electron. Similarly, for the parent molecule (CBe₄²⁻) of cluster **1**, the value of ADE is close to its VDE (2.14 vs. 1.93 eV), which suggests that it is stable structurally.

In summary, we predict dynamically stable global minima with planar tetracoordinate carbon and nitrogen atoms supported by beryllium atoms alone. Although **1** and **2** have three delocalized σ orbitals and one delocalized π orbital, there is no corresponding double aromaticity instead of anti-aromaticity. This is attributed to the fact that the stronger localized Be–Be bonds at their periphery prevent the full delocalization of electrons on the CBe₄/NBe₄ skeleton. Remarkably, they are stabilized by multicentric bonds. Meanwhile, the simulated PES spectra are given for experimentalists' reference. Given the fewer components (C–Be binary) and mono-anion, combined with the increasingly mature experimental techniques of beryllium chemistry, we believe that **1** and **2** will be observed by experimental scientists just like the milestone planar tetracoordinate clusters CAL_4^- and NAL_4^- .

Conflicts of interest

There are no conflicts to declare.

Notes and references

- (a) L. M. Yang, E. Ganz, Z. F. Chen, Z. X. Wang and P. V. R. Schleyer, *Angew. Chem., Int. Ed.*, 2015, **54**, 9468–9501 and the references therein; (b) V. Vassilev-Galindo, S. Pan, K. J. Donald and G. Merino, *Nat. Rev. Chem.*, 2018, **2**, 1–10 and the references therein.
- (a) C. Chen, Y. Liu and Z. Cui, *Inorg. Chem.*, 2021, **60**, 16053–16058; (b) M. Wang, C. Chen, S. Pan and Z. Cui, *Chem. Sci.*, 2021, **12**, 15067–15076; (c) G. Castillo-Toraya, M. Orozco-Ic, E. Dzib, X. Zarate, F. Ortíz-Chi, Z.-H. Cui, J. Barroso and G. Merino, *Chem. Sci.*, 2021, **12**, 6699–6704; (d) L. Leyva-Parra, L. Diego, O. Yañez, D. Inostroza, J. Barroso, A. Vásquez-Espinal, G. Merino and W. Tiznado, *Angew. Chem., Int. Ed.*, 2021, **60**, 8700–8704; (e) B. Jin, R. Sun, B. Huo, C. Yuan and Y. B. Wu, *Chem. Commun.*, 2021, **57**, 13716–13719.
- (a) J. O. C. Jimenez Halla, Y. B. Wu, Z. X. Wang, R. Islas, T. Heine and G. Merino, *Chem. Commun.*, 2010, **46**, 8776–8778; (b) A. I. Boldyrev and L.-S. Wang, *J. Phys. Chem. A*, 2001, **105**, 10759–10775; (c) X. Li, H.-J. Zhai and L.-S. Wang, *Chem. Phys. Lett.*, 2002, **357**, 415–419; (d) X. Li, H.-F. Zhang, L.-S. Wang, G. D. Geske and A. I. Boldyrev, *Angew. Chem., Int. Ed.*, 2000, **39**, 3630–3632.
- (a) L. S. Wang, *Int. Rev. Phys. Chem.*, 2016, **35**, 69–142; (b) L. S. Wang, H. S. Cheng and J. Fan, *J. Chem. Phys.*, 1995, **102**, 9480–9493.
- (a) X. Li, L.-S. Wang, A. I. Boldyrev and J. Simons, *J. Am. Chem. Soc.*, 1999, **121**, 6033–6038; (b) A. I. Boldyrev, X. Li and L. S. Wang, *Angew. Chem., Int. Ed.*, 2000, **39**, 3445–3448.
- (a) P. V. R. Schleyer and A. I. Boldyrev, *J. Chem. Soc., Chem. Commun.*, 1991, 1536–1538; (b) S. K. Nayak, B. K. Rao, P. Jena, X. Li and L. S. Wang, *Chem. Phys. Lett.*, 1999, **301**, 379–384.
- (a) Y. B. Wu, J. L. Jiang, H. G. Lu, Z. X. Wang, N. Perez-Peralta, R. Islas, M. Contreras, G. Merino, J. I. C. Wu and P. V. R. Schleyer, *Chem. – Eur. J.*, 2011, **17**, 714–719; (b) C. J. Zhang, P. Wang, X. L. Xu, H. G. Xu and W. J. Zheng, *Phys. Chem. Chem. Phys.*, 2021, **23**, 1967–1975.
- (a) Y. B. Wu, Y. Duan, H. G. Lu and S. D. Li, *J. Phys. Chem. A*, 2012, **116**, 3290–3294; (b) X. F. Zhao, J. H. Bian, F. Huang, C. Yuan, Q. Wang, P. Liu, D. Li, X. Wang and Y. B. Wu, *RSC Adv.*, 2018, **8**, 36521–36526; (c) A. C. Castro, G. Martínez Guajardo, T. Johnson, J. M. Ugalde, Y. B. Wu, J. M. Mercero, T. Heine, K. J. Donald and G. Merino, *Phys. Chem. Chem. Phys.*, 2012, **14**, 14764–14768; (d) Q. Luo, *Sci. China, Ser. B: Chem.*, 2008, **51**, 1030–1035; (e) R. Grande Aztatz, J. L. Cabellos, R. Islas, I. Infante, J. M. Mercero, A. Restrepo and G. Merino, *Phys. Chem. Chem. Phys.*, 2015, **17**, 4620–4624; (f) J. C. Guo, L. Y. Feng, J. Barroso, G. Merino and H. J. Zhai, *Chem. Commun.*, 2020, **56**, 8305–8308; (g) J. C. Guo, G. M. Ren, C. Q. Miao, W. J. Tian, Y. B. Wu and X. Wang, *J. Phys. Chem. A*, 2015, **119**, 13101–13106.
- Z. Chen, C. S. Wannere, C. Corminboeuf, R. Puchta and P. V. R. Schleyer, *Chem. Rev.*, 2005, **105**, 3842–3888.
- (a) X. F. Zhao, J. J. Li, H. R. Li, C. Yuan, X. Tian, S. D. Li, Y. B. Wu, J. C. Guo and Z. X. Wang, *Phys. Chem. Chem. Phys.*, 2018, **20**, 7217–7222; (b) J. C. Guo, L. Y. Feng, C. Dong and H. J. Zhai, *J. Phys. Chem. A*, 2018, **122**, 8370–8376; (c) J. C. Guo, L. Y. Feng, C. Dong and H. J. Zhai, *Phys. Chem. Chem. Phys.*, 2019, **21**, 22048–22056.
- B. Jin, J. H. Bian, X. F. Zhao, C. X. Yuan, J. C. Guo and Y. B. Wu, *Chin. J. Struct. Chem.*, 2022, **41**, 218–226.
- M. J. Frisch, G. W. Trucks and H. B. Schlegel, *et al.*, *Gaussian 16 (Revision A.03)*, Gaussian, Inc., Wallingford, CT, 2016.
- P. Pykkö, *J. Phys. Chem. A*, 2015, **119**, 2326–2337.
- (a) M. Saunders, *J. Comput. Chem.*, 2004, **25**, 621–626; (b) P. P. Bera, K. W. Sattelmeyer, M. Saunders, H. F. Schaefer

- and P. V. R. Schleyer, *J. Phys. Chem. A*, 2006, **110**, 4287–4290; (c) The stochastic search algorithm was performed as coded in GXYZ 2.0 program^{14d,e}; (d) Y. B. Wu, H. G. Lu, S. D. Li and Z. X. Wang, *J. Phys. Chem. A*, 2009, **113**, 3395–3402; (e) H. G. Lu and Y. B. Wu, *GXYZ 2.0*, Shanxi University, Taiyuan, 2015.
- 15 H. J. Werner and P. J. Knowles, *J. Chem. Phys.*, 1988, **89**, 5803–5814.
- 16 (a) The BOMD simulations were performed at the PBE^{16b}/DZVP^{16c} level using the CP2K package^{16d}; (b) J. P. Perdew, K. Burke and M. Ernzerhof, *Phys. Rev. Lett.*, 1996, **77**, 3865–3868; (c) J. VandeVondele and J. Hutter, *J. Chem. Phys.*, 2007, **127**, 114105; (d) T. D. Kühne and J. Hutter, *J. Chem. Phys.*, 2020, **152**, 194103.
- 17 D. Y. Zubarev and A. I. Boldyrev, *Phys. Chem. Chem. Phys.*, 2008, **10**, 5207–5217.
- 18 (a) P. v R. Schleyer, C. Maerker, A. Dransfeld, H. Jiao and N. J. R. V. E. Hommes, *J. Am. Chem. Soc.*, 1996, **118**, 6317–6318; (b) Z. Chen, C. S. Wannere, C. Corminboeuf, R. Puchta and P. V. R. Schleyer, *Chem. Rev.*, 2005, **105**, 3842–3888.
- 19 (a) The ICSSs were generated with the Multiwfn 3.8 code^{19b}; (b) T. Lu and F. Chen, *J. Comput. Chem.*, 2012, **33**, 580–592.
- 20 (a) B. M. Wong and J. G. Cordaro, *J. Phys. Chem. C*, 2011, **115**, 18333–18341; (b) D. Zhao, X. He, M. Li, B. Wang, C. Guo, C. Rong, P. K. Chattaraj and S. Liu, *Phys. Chem. Chem. Phys.*, 2021, **23**, 24118–24124.